# UAV-Assisted Data Collection with Non-Orthogonal Multiple Access

Weichao Chen[1,2,3], Shengjie Zhao[1,3], Rongqing Zhang[1,2], and Liuqing Yang[4]
[1]School of Software Engineering, Tongji University, Shanghai, China,
[2]National Mobile Communications Research Laboratory, Southeast University, China
[3]Key Laboratory of Embedded System and Service Computing, Ministry of Education, Tongji University, Shanghai, China
[4]Department of Electrical & Computer Engineering, Colorado State University, CO, USA.
{carlyle.chen, shengjiezhao, rongqingz@tongji.edu.cn, lqyang@engr.colostate.edu}

***Abstract*—Unmanned aerial vehicles (UAVs) facilitate information collection greatly in Internet of Things (IoT) systems. On the other hand, non-orthogonal multiple access (NOMA) is regarded as a promising technology to provide high spectral efficiency and support massive connectivity in 5G networks. The integration of NOMA into UAV-assisted wireless networks shows great potential, but how to determine the user grouping and power allocation in NOMA according to the different locations of UAV is challenging. In this paper, we propose a general NOMA-enabled UAV-assisted data collection (NUDC) protocol to solve the formulated sum rate maximization problem such that the location of UAV, sensor grouping, and power control are jointly considered. Moreover, a joint signal-to-interference-ratio (SIR) hypergraph-based grouping and power control (SHG-PC) NOMA scheme is provided to obtain the appropriate sensor grouping and the optimal power control solutions efficiently. Extensive simulation results demonstrate the effectiveness of our proposed protocol.**

***Index Terms*—UAV, data collection, NOMA.**

## I. Introduction

UAV-assisted communications has been recognized as an emerging technique for its superior flexibility and mobility. Generally speaking, there are three main typical UAV-assisted communication scenarios [1], where UAVs are served as aerial base stations [2, 3], relays [4, 5], and information disseminators or data collectors. Due to the fully controllable mobility, UAVs become especially helpful as data collectors to get access to the remote sensors in IoT systems (e.g., ocean observation network). Many researches [6, 7] on UAV-assisted information collection have obtained performance gains by optimizing the trajectory or position of the UAV, combined with the mature orthogonal multiple access (OMA) technology. However, with the increasing communication requirements of users or devices, the limited spectrum resources is continuously exhausting. To further integrate UAVs into the IoT scenarios, enhanced multiple access techniques are essential.

Non-orthogonal multiple access (NOMA) [8, 9] has been regarded as a promising candidate in the fifth generation (5G) and beyond 5G (B5G) networks for providing high spectral efficiency and supporting massive connectivity. Different from traditional OMA, NOMA serves multiple users on the same resource block (time/frequency/code/space) but with different power levels in terms of users' respective channel gain differences. Then, at the receivers, successive interference cancellation (SIC) is applied for multi-user detection and decoding. As a result, NOMA is capable of enhancing connectivity and allows serving individual users with higher effective bandwidth [10, 11]. For this reason, the integration of NOMA into UAV-assisted wireless networks shows great potential in future communication networks. In [12], the authors optimized the UAV placement and power allocation (PA) to improve the average sum rate performance. A PA strategy for NOMA was proposed in [13] to maximize the sum rate of a simple two-user network with a fixed UAV coordinate, which does not fully exploit the mobility of the UAV.

The combination of UAVs and NOMA can definitely promote the flexibility and efficiency of data collection in IoT scenarios. However, in the aforementioned works, the problem of user grouping and power optimization for NOMA in UAV-assisted communication networks has not been well researched. Therefore, in this paper, we investigate a UAV-assisted uplink NOMA system where a UAV is employed to collect data with NOMA. One should note that different locations of the UAV lead to various differences in large-scale channel gains of UAV-to-ground links, and thus will have a great effect on the user grouping and power allocation in NOMA. Hence, in order to better exploit both the mobility of the UAV and the efficiency of NOMA to improve the UAV-assisted data collection performance, we formulate a joint optimization problem of the location of UAV, sensor grouping, and power control in terms of system sum rate. Then, we propose a general NOMA-enabled UAV-assisted data collection (NUDC) protocol to solve the formulated problem, which can obtain the optimal placement of UAV and achieve performance gains with NOMA. Extensive simulation results demonstrate our NUDC protocol can not only provide the optimal placement of UAV, but also perform like a hybrid approach that can leverage the benefits of both NOMA and OMA, thereby achieving performance gains. The rest of the paper is organized as follows. Section II introduces the system model and the problem formulation for a general UAV-assisted uplink NOMA system. Section III presents the detailed solutions of the proposed NUDC protocol. Section IV evaluates the performances numerically and Section V concludes the paper.

978-1-7281-3106-1/20/$31.00 ©2020 IEEE

## II. System Model and Problem Formulation

### A. System Model

As shown in Fig. 1, we consider a UAV-assisted uplink NOMA system with a single UAV serving as a data collector for a set $\mathcal{K} \triangleq \{1, ..., K\}$ of buoy sensors. Multiple sensors are involved in one NOMA group to improve the spectrum efficiency, despite the existence of mutual interference. The sensors within one NOMA group transmit data to the UAV non-orthogonally over the same frequency resource block (RB). Each NOMA group uses several frequency RBs that is orthogonal to other RBs. The buoy sensors are distributed uniformly and each sensor is requested to upload its sensing data under the constraint of maximum transmit power $P_{max}$.

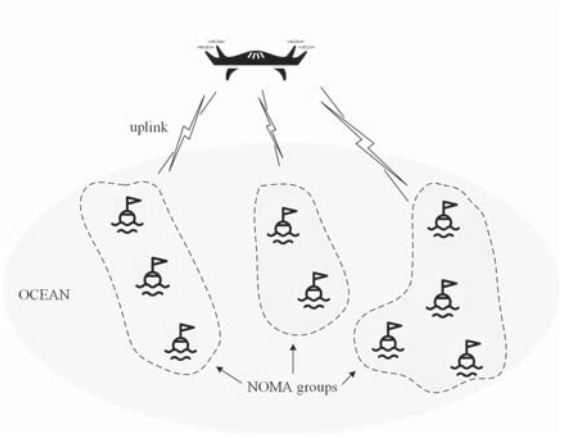


Fig. 1: A UAV-assisted uplink NOMA system.

Without loss of generality, we consider a 3D Cartesian coordinate system where the horizontal coordinate of buoy sensor $k$ is fixed at $(x_k, y_k)$. The UAV's horizontal coordinate is $(x_U, y_U)$ and its flight altitude is $H$. As mentioned above, the communication links from the sensors to the UAV are dominated by LOS where the channel attenuation mainly depends on the sensor-UAV distance. Thus, the channel gain $g_k$ between the $k$-th sensor and the UAV can be given by

$$g_k = \rho_0 d_k^{-2} = \frac{\rho_0}{(x_U - x_k)^2 + (y_U - y_k)^2 + H^2}, \forall k, \quad (1)$$

where $d_k$ is the distance between the UAV and sensor $k$ and $\rho_0$ denotes the channel power gain at the reference distance $d_0 = 1$m. We assume that the channel gains follow $g_1 \geq ... \geq g_k \geq ... \geq g_K > 0$. Therefore, the achievable rate for sensor $k$ in a NOMA group can be presented as

$$R_k = \omega B_0 \log_2 \left(1 + \frac{p_k g_k}{\sum_{j=k+1}^{K} p_j g_j + \omega B_0 N_0}\right), \forall k, \quad (2)$$

where $\omega$ is the total number of RBs, $B_0$ is the bandwidth of each block, $N_0$ is the noise power spectral density, and $p_k$ is the transmit power of sensor $k$. Given the system available bandwidth $B_A$, the total number of RBs $\omega$ can be calculated by $B_A/B_0$.

Obviously, each NOMA group may contain $N = 2, 3, ..., K$ sensors and the number of groups ranges between 1 and $K/2$. To represent sensor grouping, we define a binary variable $\alpha_{k,l}$ to indicate the $k$-th sensor is assigned to the $l$-th group if $\alpha_{k,l} = 1$; otherwise $\alpha_{k,l} = 0$. Note that $k = 1, 2, ..., K$ and $l = 1, 2, ..., K/2$. Therefore, we have such constraints as $\alpha_{k,l} \in \{0, 1\}, \forall k, l$ and $\sum_{l=1}^{K/2} \alpha_{k,l} = 1, \forall k$ to ensure each sensor can be assigned to at most one group.

As a result, the achievable rate of sensor $k$ belonging to the $l$-th group can be given as

$$R_{k,l} = \alpha_{k,l}\omega_l B_0 \log_2 \left(1 + \frac{p_k g_k}{\alpha_{j,l} \sum_{j=k+1}^{K} p_j g_j + \omega_l B_0 N_0}\right), \forall k, l, \quad (3)$$

where $\omega_l$ denotes the number of RBs of the $l$-th group, and $\sum_{l=1}^{K/2} \omega_l = \omega$.

Each sensor transmits its own signal to the UAV receiver independently, despite the interference from other sensors. The UAV receives all the signals at the same time and applies SIC to decode all desired signals. Note that, to make SIC decoding process more efficient, the arrived power of each sensor $p_k g_k$ has to be distinct from that of other sensors. Then, the constraints to ensure the efficient SIC at the UAV can be expressed as

$$p_k g_k \alpha_{k,l} / (\sum_{j=k+1}^{K} p_j g_j \alpha_{j,l}) \geq \eta_{SIC}, \forall k, \quad (4)$$

where $\eta_{SIC}$ denotes the minimum power difference required for SIC.

### B. Problem Formulation

For ease of notation, let $\mathbf{X} = \{\alpha_{k,l}, \forall k, l\}$ represent the grouping set and $\boldsymbol{p} = \{p_k, \forall k\}$ represent the vector of the transmit power of all sensors. Our aim is to maximize the sum rate of the UAV-assisted uplink NOMA system by jointly optimizing the location of the UAV, sensor grouping and power control, which can be formulated as

$$(\text{P1}): \max_{x_U, y_U, \mathbf{X}, \boldsymbol{p}} \sum_{l=1}^{K/2} \sum_{k=1}^{K} R_{k,l} \quad (5)$$

$$\text{s.t.} \quad \sum_{l=1}^{K/2} R_{k,l} \geq r_k, \forall k, \quad (6)$$

$$p_k g_k \alpha_{k,l} / (\sum_{j=k+1}^{K} p_j g_j \alpha_{j,l}) \geq \eta_{SIC}, \forall k, \quad (7)$$

$$\alpha_{k,l} \in \{0, 1\}, \forall k, l, \quad (8)$$

$$\sum_{l=1}^{K/2} \alpha_{k,l} = 1, \forall k, \quad (9)$$

$$p_k \leq P_{max}, \forall k, \quad (10)$$

where $r_k$ is the minimum uplink rate requirement for the $k$-th sensor. In the formulated problem, the constraint (7) accounts for effective SIC decoding condition, and the constraint (10) limits the transmit power of all sensors.

## III. NOMA-enabled UAV-assisted Data Collection Protocol

In this section, we propose a general NOMA-enabled UAV-assisted data collection (NUDC) protocol to solve the problem (P1). As mentioned above, we decouple the problem into three sub-problems. After optimizing the location of the UAV, we propose a joint SHG-PC NOMA scheme to obtain the appropriate sensor grouping and the optimal power control solutions efficiently. The overall procedure for solving the problem (P1) is shown in Fig. 2.

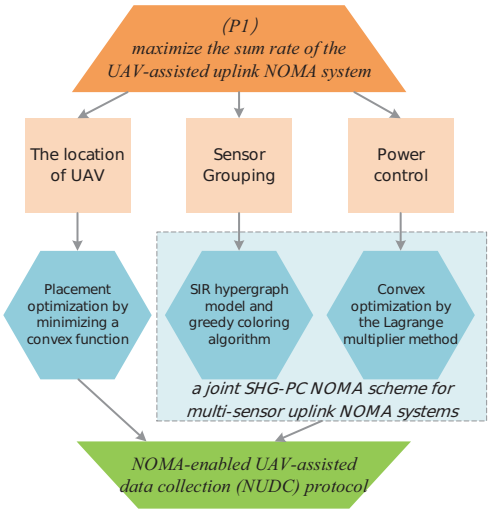


Fig. 2: The NOMA-enabled UAV-assisted data collection protocol.

### A. Placement Optimization for the UAV

Given the locations of all sensors, the optimal location of the UAV in an uplink NOMA system can be optimized by solving the following problem

$$(\mathrm{P2}): \max_{x_U, y_U} B_0 \sum_{k=1}^{K} \log\left(1 + \frac{p_k \rho_0 d_k^{-2}}{\sum_{j=k+1}^{K} p_j \rho_0 d_j^{-2} + B_0 N_0}\right). \tag{11}$$

If we further expand the objective function, it can be reduced to the following problem

$$(\mathrm{P3}): \quad \max_{x_U, y_U} \quad B_0 \log\left(\frac{\sum_{k=1}^{K} p_k \rho_0 d_k^{-2} + B_0 N_0}{B_0 N_0}\right), \tag{12}$$

since the achievable data rate for the $K$-th sensor is $R_K = \log\left(1 + \frac{p_K \rho_0 d_K^{-2}}{B_0 N_0}\right)$.

In addition, according to the theorem that the harmonic mean is less than the arithmetic mean, we obtain

$$\frac{\sum_{k=1}^{K} d_k^{-2}}{K} \geq \frac{K}{\sum_{k=1}^{K} d_k^2}. \tag{13}$$

Therefore, (P3) can be further rewritten as

$$(\mathrm{P4}): \quad \min_{x_U, y_U} \quad \sum_{k=1}^{K} (x_U - x_k)^2 + (y_U - y_k)^2, \tag{14}$$

which means obtaining the optimal location of the UAV is equivalent to minimizing the sum distance between the UAV and the sensors. Then, Lemma III.1 provides the optimal solution of (P4) as follows.

**Lemma III.1** *The optimal solution of $x_U, y_U$ in (P4) is*

$$x_U = \sum_{k=1}^{K} x_k / K, \quad y_U = \sum_{k=1}^{K} y_k / K. \tag{15}$$

**Proof III.1** *Note that the objective function in (P4) is convex with respect to $x_U$ and $y_U$. The optimal solution can be obtained by letting the first-order derivative equal to zero, which can be expressed as $2Kx_U - 2\sum_{k=1}^{K} x_k = 0$ and $2Ky_U - 2\sum_{k=1}^{K} y_k = 0$. Therefore, Lemma III.1 is proved.*

### B. Hypergraph-Based Sensor Grouping

In this subsection, we propose to exploit a hypergraph [**?** ] to model the signal-to-interference-ratio (SIR) among sensors in the uplink NOMA system, and further provide an effective and efficient greedy coloring algorithm for sensor grouping.

*1) SIR Hypergraph Construction:* First, we provide a brief introduction about hypergraphs [**?** ]. A hypergraph $HG$ can be denoted as $HG = \{VX, EG\}$, where $VX$ is the set of vertices and $EG$ is the set of hyperedges. A hypergraph requires a incidence matrix to specify the relationships between vertices and hyperegdes. If vertex $vx_i$ is incident to hyperedge $eg_j$, then $(i; j)$-entry in the incidence matrix is set as 1, otherwise 0. The degree of the vertex $vx$ is defined as the number of the hyperedges associating with the vertex $vx$, which can be denoted by $|D(vx)|$.

Therefore, if we represent the sensors as vertices and the NOMA groups they formed as hyperedges in a hypergraph, the non-zero elements in the incidence matrix can represent the affiliations of the sensors and the candidate groups. The criteria of forming a candidate group should be determined by the overall QoS, which means the mutual interference in a NOMA group should be small enough to satisfy the transmission and decoding conditions. We propose to construct a SIR hypergraph that each sensor is represented by a vertex, and a hyperedge is constructed with sensor $k$ and all other $N-1$ sensors if Eq. (16) is satisfied.

$$\frac{p_k g_k}{\sum_{\varkappa}^{N-1} p_\varkappa g_\varkappa} \geq \eta, \forall k, \tag{16}$$

where $\varkappa \in \mathcal{K}$ denotes a subset of sensors that contains $N-1$ sensors and $\eta$ denotes the threshold of SIR. The threshold $\eta$ needs to be determined properly since a high threshold results in too few candidate NOMA groups, whereas a low threshold makes the channel gains of the sensors involved in the same group less discriminative. $N$ is the maximum number of vertices considered in hyperedge construction. In this paper, we consider the hyperedges with at most six vertices for simplicity, which means $N = 6$.

Based on the above discussion, the construction flow of the hypergraph iteratively judges whether the SIR condition

is satisfied, which will mark all the candidate NOMA groups as hyperedges. By denoting the $N$-sensor subset with $\mathcal{N}$, the overall algorithm for SIR hypergraph construction is summarized in Algorithm 1.

**Algorithm 1** SIR hypergraph construction

Input: Given channel gains $g_k, \forall k$ and the transmit power $p_k, \forall k$, $N = 6$.
**repeat**
  **repeat**
    Select a subset $\mathcal{N}$
    **if** Eq.(16) is satisfied **then**
      Construct a hyperedge among $N$ sensors
    **end if**
  **until** Each subset has been traversed.
  Update $N = N - 1$
**until** $N = 2$
Output: A constructed SIR hypergraph.

*2) Sensor Grouping with Greedy Coloring Algorithm:*

**Definition III.1** *In a hypergraph $HG(VX, EG)$, delete a hyperedge $eg \in EG$ from $HG$ means to remove all the vertices contained in $eg$ and any hyperedge connected to them.*

In the greedy coloring algorithm, the main process can be summarized as follows: First, sort the vertices by the degrees $|D(vx)|$ of the vertices and select the vertex $vx$ with the minimum degree from the hypergraph $HG$. Then, find the maximum hyperedge $eg$ containing $vx$ and color all the vertices in $eg$ with one color. After that, delete the $eg$ to form a new induced sub-hypergraph and repeat the selection of the vertex with the minimum degree until every vertex in the hypergraph is colored. The detailed procedure of the greedy coloring algorithm is given in Algorithm 2. Coloring the constructed hypergraph from the vertex with minimum degree can prevent the vertex from being left alone, which allows the sensor with the worst channel gain being assigned into a group with a high bandwidth.

**Algorithm 2** Hypergraph coloring algorithm

Input: Given a hypergraph constructed by Algorithm 1.
Initialization: Set $k = K$,$HG_k = HG$. Find the vertex $vx_k$ which has the minimum degree in $HG_k$.
**repeat**
  Find the maximum hyperedge $eg_k$ containing $vx_k$ .
  Color all vertices in $eg_k$ with one color.
  Delete $eg_k$ from $HG_k$ and form the induced sub-hypergraph, $HG_{k-1} = HG_k - eg_k$.
  Find the vertex $vx_{k-1}$ which has the minimum degree in $HG_{k-1}$.
  Update $k = k - 1$
**until** $k = 1$
Output: A colored SIR hypergraph.

### C. Power Control in Uplink NOMA

Given the NOMA groups obtained from the last subsection, we derive the closed-form power control solution for an uplink NOMA group with $n$ sensors, where $2 \le n \le N$. The power control sub-problem can be expressed as

$$(\mathrm{P5}): \quad \max_{\boldsymbol{p}} B_0 \sum_{k=1}^{n} \log\left(1 + \frac{p_k g_k}{\sum_{j=k+1}^{n} p_j g_j + B_0 N_0}\right) \tag{17}$$

$$\text{s.t.} \quad B_0 \log\left(1 + \frac{p_k g_k}{\sum_{j=k+1}^{n} p_j g_j + B_0 N_0}\right) \ge r_k, \quad \forall k = 1, 2, ..., n, \tag{18}$$

$$p_k g_k / (\sum_{j=k+1}^{n} p_j g_j) \ge \eta_{SIC}, \forall k = 1, 2, ..., n-1, \tag{19}$$

$$p_k \le P_{max}, \forall k = 1, 2, ..., n, \tag{20}$$

Note that the above optimization problem is convex under the listed constraints, and thus we could address it by applying the Lagrange multiplier method. The Lagrange function of the above problem can be expressed as

$$\begin{aligned}\mathcal{L}(\boldsymbol{p}, \boldsymbol{\lambda}, \boldsymbol{\mu}, \boldsymbol{\psi}) &= B_0 \sum_{k=1}^{n} \log\left(1 + \frac{p_k g_k}{\sum_{j=k+1}^{n} p_j g_j + B_0 N_0}\right) \\ &+ \sum_{k=1}^{n} \mu_k (p_k g_k - \sum_{j=k+1}^{n} \phi_k p_j g_j - \phi_k B_0 N_0) \\ &+ \sum_{k=1}^{n} \psi_k (p_k g_k - \eta_{SIC} \sum_{j=k+1}^{n} p_j g_j) + \sum_{k=1}^{n} \lambda_k (P_{max} - p_k),\end{aligned} \tag{21}$$

where $\phi_k = (2^{r_k/B_0} - 1)$, and $\lambda_k, \mu_k, \psi_k$ are the Lagrange multipliers. Taking derivatives of (21) with regards to $p_k, \lambda_k, \mu_k$ and $\psi_k$, we obtain

$$\begin{aligned}\frac{\partial \mathcal{L}}{\partial p_k^*} &= \frac{B_0 g_k}{\sum_{j=1}^{N} p_j g_j + B_0 N_0} - \lambda_k + \mu_k g_k - \sum_{m=1}^{k-1} \phi_m \mu_m g_k \\ &+ g_k \psi_k - \eta_{SIC} \sum_{m=1}^{k-1} \psi_m g_m, \forall k = 1, 2, ..., n,\end{aligned} \tag{22}$$

$$\frac{\partial \mathcal{L}}{\partial \lambda_k^*} = P_{max} - p_k, \forall k = 1, 2, ..., n, \tag{23}$$

$$\frac{\partial \mathcal{L}}{\partial \mu_k^*} = p_k g_k - \sum_{j=k+1}^{n} \phi_k p_j g_j - \phi_k, \forall k = 1, 2, ..., n, \tag{24}$$

$$\frac{\partial \mathcal{L}}{\partial \psi_k^*} = p_k g_k - \eta_{SIC} \sum_{j=k+1}^{n} p_j g_j, \forall k = 1, 2, ...n-1. \tag{25}$$

By checking the KKT conditions of all combinations of Lagrange multipliers, we can obtain the optimal power control solutions. Note that in our problem, since the transmit power of sensors $p_k > 0, \forall k$, only three types of combinations need to be checked. Note that these combinations correspond to the constraints (18)-(20) respectively, and thus the solution set is $S = \{\lambda_1, \lambda_2, ..., \lambda_{n-1}\} \bigcup \{\lambda_n \text{ or } \mu_{n-1} \text{ or } \psi_{n-1}\}$. For example, for a 4-sensor uplink NOMA group, the satisfied KKT conditions are $S_1 = \{\lambda_1, \lambda_2, \lambda_3, \lambda_4\}$, $S_2 = \{\lambda_1, \lambda_2, \lambda_3, \mu_3\}$,

TABLE I: Simulation parameters.

| | |
|---|---|
| Simulation area | 2km×2km |
| UAV flight altitude, $H$ | 100 m |
| Bandwidth of each resource block, $B_0$ | 180 kHz |
| Channel power gain at the reference distance, $\rho_0$ | -60 dB |
| System available bandwidth, $B_A$ | 10 MHz |
| Uplink transmit power budget, $P_{max}$ | 24 dBm |
| Number of transmit/receive antenna at UAV and sensor | 1 |
| White noise power spectral density, $N_0$ | -174 dBm/Hz |
| Minimum data rate requirement, $r_k, \forall k$ | 100 kbps |

$S_3 = \{\lambda_1, \lambda_2, \lambda_3, \psi_3\}$. Then, the closed-form solutions of power control for an $n$-sensor uplink NOMA group can be given as follows:
(i) if $S$ contains $\mu_{n-1}$, $p_k = P_{max}, \forall k = 1, 2, ..., n-1$, $p_n = (P_{max} g_{n-1} - \phi_{n-1})/(\phi_{n-1} g_n)$;
(ii) if $S$ contains $\psi_{n-1}$, $p_k = P_{max}, \forall k = 1, 2, ..., n-1$, $p_n = P_{max} g_{n-1}/(\eta_{SIC} g_n)$;
(iii) otherwise $p_k = P_{max}, \forall k$.

## IV. Numerical Results

In this section, we investigate the sum rate performance of UAV-assisted uplink NOMA system with our proposed NUDC protocol. The major simulation parameters are shown in **Table 1**.

The locations of the UAV and buoy sensors are shown in Fig. 3, where 4 sensors are randomly distributed in an ocean area of 2km × 2km, which are marked by red circles. Three locations are selected for the UAV. The blue pentagram is the optimal location obtained according to Lemma 1. The other two green squares are the randomly chosen locations for the UAV. The sum rate of the system is compared in Fig. 4 for different values of transmit power budget. In Fig. 4, we can observe that the sum rate increases with the transmit power of the sensors and the performance of the location optimized according to Lemma III.1 is always better than that of the randomly selected locations.

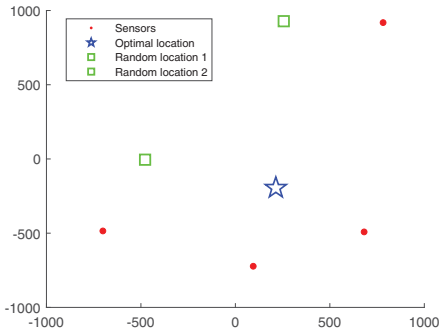


Fig. 3: Simulation area.

After determining the optimal location of the UAV, we compare the sum rate performance of our proposed scheme with the 1) 4-sensor NOMA, 2) 3-sensor NOMA, and 3) 2-sensor NOMA schemes proposed in [11]. Note that in any scheme, if power control does not meet the minimum rate

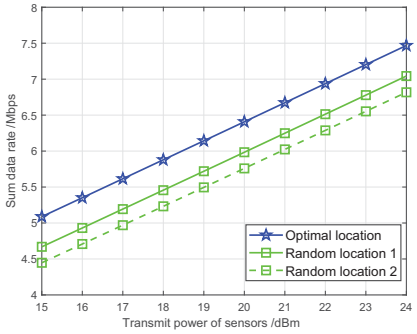


Fig. 4: Sum rate comparison with random locations.

requirements, the sensors will transmit data in the OMA mode. Fig. 5 and Fig. 6 provide the average sum rate performance comparison in which each $\eta$ is simulated for 1000 times and the number of sensors is 12.

In Fig. 5, we compare the sum rate performance of our SHG-PC NOMA scheme with the other three schemes by setting the minimum power of difference $\eta_{SIC}$ as 5 dB. It can be observed that the sum rate of our proposed scheme is higher than the other three schemes when the value of SIR threshold $\eta$ is close to $\eta_{SIC}$. This result is within our expectation since a low SIR threshold $\eta$ causes the channel gains of sensors in one NOMA group are less discriminative whereas a high $\eta$ makes it difficult to form candidate groups. An appropriate $\eta$ that is close to $\eta_{SIC}$ are more likely to form the ideal NOMA group in which the inter-sensor interference can be effectively controlled.

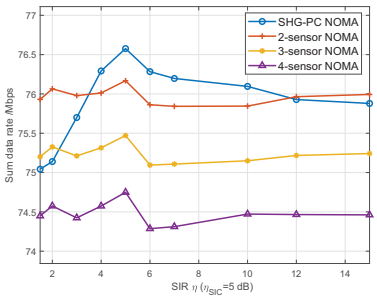


Fig. 5: Sum rate comparison with $\eta_{SIC} = 5$ dB.

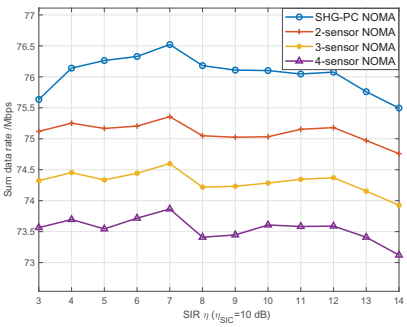


Fig. 6: Sum rate comparison with $\eta_{SIC} = 10$ dB.

When the value of $\eta_{SIC}$ is set as 10 dB, we observe that our proposed scheme outperforms the three schemes totally in Fig. 6. Since the SIC decoding condition is more stringent than before, there exists severe inter-sensor interference in the NOMA groups formed by the three schemes. Our SHG-PC NOMA scheme can actively select the sensors suitable for NOMA transmission to form groups and arrange other sensors transmit data in the OMA mode. In this case, the scheme we proposed performs like a hybrid approach that can leverage the strengths of both NOMA and OMA.

In Fig. 7, we compare our proposed scheme with the 2-sensor NOMA scheme to investigate the impact of the number of sensors. Fig. 7 shows that when the number of sensors is small (6 or 8), the performance of the 2-sensor NOMA scheme is a litter better than our scheme. As the number of sensors grows (10 and more), our scheme goes beyond. The reason is that in such a fixed-size area, the channel gains of sensors are likely to be less discriminative with the increase of the quantity of sensors. When the number of sensors is large, arbitrary grouping may result in a significant performance degradation due to the severe inter-sensor interference within the NOMA group. Our SHG-PC NOMA scheme is able to evade the risk of inter-sensor interference by selecting some of the sensors that are suitable for NOMA transmission, and thus improve the overall performance.

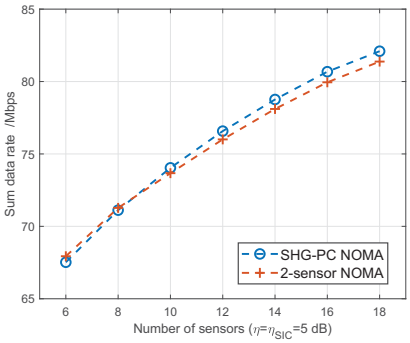


Fig. 7: Sum rate comparison with different number of sensors.

## V. Conclusion

In this paper, we have investigated a UAV-assisted uplink NOMA system that the UAV is employed to collect data from multiple sensors with NOMA. A general NOMA-enabled UAV-assisted data collection (NUDC) protocol has been proposed for solving the formulated sum rate maximization problem. We decoupled the formulated problem into three sub-problems of the placement of UAV, sensor grouping, and power control, and then solved them separately. Extensive performance evaluations have demonstrated that our NUDC protocol not only provides the optimal location for the UAV in data collection, but also effectively reduces the inter-sensor interference and forms appropriate NOMA groups, thereby achieving the performance gains.

## VI. Acknowledgment

This work was supported in part by the National Natural Science Foundation of China under Grants 61936014 and 61901302, in part by the National Key Research and Development Project under Grant 2019YFB2102300, 2019YFB2102301, and 2017YFE0119300. This work was also supported in part by the open research fund of National Mobile Communications Research Laboratory, Southeast University (No. 2020D01), in part by the Scientific Research Project of Shanghai Science and Technology Committee under Grant 19511103302, and in part by the National Science Foundation under Grant CPS-1932413 and ECCS-1935915.

## References

[1] Y. Zeng, R. Zhang, and T. J. Lim,"Wireless Communications with Unmanned Aerial Vehicles: Opportunities and Challenges," *IEEE Commun. Mag.*, vol. 54, no. 5, pp. 36–42, May. 2016.

[2] J. Lyu, Y. Zeng, R. Zhang, and T. J. Lim,"Placement Optimization of UAV-Mounted Mobile Base Stations," *IEEE Commun. Lett.*, vol. 21, no. 3, pp. 604–607, Mar. 2017.

[3] R. I. Bor-Yaliniz, A. El-Keyi, and H. Yanikomeroglu,"Efficient 3-D Placement of An Aerial Base Station in Next Generation Cellular Networks," in *Proc. IEEE Int. Conf. Commun. (ICC)*, 2016, pp. 1–5.

[4] Y. Zeng, R. Zhang, and T. J. Lim,"Throughput Maximization for UAV-Enabled Mobile Relaying Systems," *IEEE Trans. Commun.*, vol. 64, no. 12, pp. 4983–4996, Dec. 2016.

[5] W. Chen, S. Zhao, and Q. Shi, "Improve Stability in UAV Relay Networks by Jointly Optimizing Communication, Trajectory and Power," in *Proc. IEEE Int. Conf. Commun. Syst. (ICCS)*, 2018, pp. 180–185.

[6] Q. Wu, Y. Zeng, and R. Zhang, "Joint Trajectory and Communication Design for UAV-Enabled Multiple Access," in *Proc. IEEE Global Telecommun. Conf. (GLOBECOM)*, 2017, pp. 1–6.

[7] W. Chen, S. Zhao, Q. Shi, and R. Zhang, "Resonant Beam Charging-Powered UAV-Assisted Sensing Data Collection," *IEEE Trans. Veh. Technol*, vol. 69, no. 1, pp. 1086–1090, Jan. 2020.

[8] Z. Ding *et al.*, "Application of Non-Orthogonal Multiple Access in LTE and 5G Networks," *IEEE Commun. Mag.*, vol. 55, no. 2, pp. 185–191, Feb. 2017.

[9] A. Benjebbovu *et al.*, "System-Level Performance of Downlink NOMA for Future LTE Enhancements," in *Proc. IEEE Globlecom Workshop*, Atlanta, GA, USA, Dec. 2013, pp. 66–70.

[10] Z. Ding, X. Lei, G. K. Karagiannidis, R. Schober, J. Yuan, and V. K. Bhargava, "A Survey on Non-Orthogonal Multiple Access for 5G Networks: Research Challenges and Future Trends," *IEEE J. Sel. Areas Commun.*, vol. 35, no. 10, pp. 2181–2195, Oct. 2017.

[11] M. S. Ali, H. Tabassum, and E. Hossain, "Dynamic User Clustering and Power Allocation for Uplink and Downlink Non-Orthogonal Multiple Access (NOMA) Systems," *IEEE Access*, vol. 4, pp. 6325–6343, 2016.

[12] X. Liu *et al.*, "Placement and Power Allocation for NOMA-UAV Networks," *IEEE Wireless Commun. Lett.*, vol. 8, no. 3, pp. 965–968, Jun. 2019.

[13] M. F. Sohail, C. Y. Leow, and S. Won, "Non-Orthogonal Multiple Access for Unmanned Aerial Vehicle Assisted Communication," *IEEE Access*, vol. 6, pp. 22716–22727, 2018.

[14] C. Chen, B. Wang, and R. Zhang, "Interference Hypergraph-Based Resource Allocation (IHG-RA) for NOMA-Integrated V2X Networks," *IEEE Internet of Things Journal*, vol. 6, no. 1, pp. 161–170, Feb. 2019.

[15] B. Wang, R. Zhang, C. Chen, X. Cheng, L. Yang, and Y. Jin, "Interference Hypergraph-Based 3D Matching Resource Allocation Protocol for NOMA-V2X Networks," *IEEE Access,* vol. 7, pp. 90789–90800, 2019.